



Solubility and hydrolysis of Tc(IV) in dilute to concentrated KCl solutions: an extended thermodynamic model for Tc⁴⁺–H⁺–K⁺–Na⁺–Mg²⁺–Ca²⁺–OH[–]–Cl[–]–H₂O(l) mixed systems

A. Baumann, * E. Yalçıntaş, X. Gaona, * M. Altmaier and H. Geckeis

The solubility of ⁹⁹Tc(IV) under strongly reducing conditions ($p_e + \text{pH}_m = 2$, with $\text{pH}_m = -\log[\text{H}^+]$) is investigated in KCl solutions of different ionic strengths ($I = 0.1, 0.5, 3.0$ and 4.0 M) at $1.5 \leq \text{pH}_m \leq 14.5$. Undersaturation solubility experiments were conducted in an Ar-glovebox ($\text{O}_2 \leq 1$ ppm) at $T = (22 \pm 2)$ °C. Liquid–liquid extraction confirmed that the redox state of Tc was kept as +IV during the timeframe of the experiments (≤ 500 days). Solid phase characterization performed by XRD, SEM-EDS, quantitative chemical analysis and TG-DTA confirmed that $\text{TcO}_2 \cdot 0.6\text{H}_2\text{O}(\text{s})$ controls the solubility of Tc(IV) under the conditions investigated. Experimental solubility data determined at $1 \leq \text{pH}_m \leq 10$ are properly explained assuming the predominance of $\text{Tc}_3\text{O}_5^{2+}$ and $\text{TcO}(\text{OH})_2(\text{aq})$ in the aqueous phase, and considering thermodynamic and activity models recently reported in the literature for these species. Above $\text{pH}_m \geq 10$, the combination of solid phase characterization with slope analysis of solubility data indicates a solubility control by the chemical reaction $\text{TcO}_2 \cdot 0.6\text{H}_2\text{O}(\text{s}) + 1.4\text{H}_2\text{O}(\text{l}) \rightleftharpoons \text{TcO}(\text{OH})_3 + \text{H}^+$. The hydrolysis constant and SIT/Pitzer ion interaction coefficients of $\text{TcO}(\text{OH})_3$ with K^+ have been determined in the present work. Additional solubility experiments with $\text{TcO}_2 \cdot 0.6\text{H}_2\text{O}(\text{s})$ in mixed alkaline KCl–NaCl–MgCl₂–CaCl₂ electrolyte solutions of specific relevance in the context of nuclear waste disposal show excellent agreement with thermodynamic calculations using thermodynamic and activity models derived in our group for the system Tc^{4+} – H^+ – K^+ – Na^+ – Mg^{2+} – Ca^{2+} – OH^- – Cl^- – $\text{H}_2\text{O}(\text{l})$.

1. Introduction

Technetium-99 is one of the main fission products of ²³⁵U and ²³⁹Pu in nuclear reactors. Due to its long half-life (2.1×10^5 a) and redox-sensitive chemical behavior, ⁹⁹Tc is an important radionuclide in Performance Assessment (PA) exercises of repositories for the final disposal of radioactive waste. Tc can be present in different oxidation states, with Tc(VII) and Tc(IV) being those with greater relevant stability fields within the stability field of water. Tc(VII) prevails in aqueous systems under oxidizing to mildly reducing conditions, forming the very soluble and highly mobile TcO_4^- aqueous species. Under the reducing conditions expected in deep underground repositories, ⁹⁹Tc is expected to be Tc(IV) which forms the sparingly soluble hydrous oxide $\text{TcO}_2 \cdot x\text{H}_2\text{O}(\text{s})$ according to the redox equilibrium $\text{TcO}_4^- + 4\text{H}^+ + 3\text{e}^- \rightleftharpoons \text{TcO}_2 \cdot x\text{H}_2\text{O}(\text{s}) + (2 - x)\text{H}_2\text{O}(\text{l})$.

Potassium is an ubiquitous cation in surface- and groundwaters. In the context of repositories for nuclear waste disposal,

potassium becomes especially relevant in cementitious environments related to repositories for low and intermediate level radioactive waste (L/ILW), or in specific cases for high level waste (HLW, e.g. the Belgium concrete supercontainers¹). Cement-based materials are used for the conditioning of the waste components, but also as engineered barriers (container, backfill and liner materials). Studies investigating the early stages of cement degradation report the solubilisation of K_2O and Na_2O leading to hyper-alkaline aqueous systems ($\text{pH} \geq 13.3$) with a dominant presence of Na^+ and K^+ in pore water.^{2,3} Long-term experiments with cemented waste in simulated salt-rock formations showed that potassium concentrations in saline cementitious environments elevate up to 0.6 M.⁴ A high potassium concentration (0.437 M) is also considered in the Generic Weep Brine (GWB), which represents a simulated groundwater composition for the Waste Isolation Pilot Plant (WIPP) in Carlsbad (New Mexico, USA) located in a deep salt basin.^{5,6}

The Nuclear Energy Agency Thermochemical Database (NEA-TDB) provides a very comprehensive selection of equilibrium constants for solubility, hydrolysis, redox and complexation reactions of technetium.^{7,8} After a critical review of the available experimental data, the NEA-TDB selected TcO^{2+} , $\text{TcO}(\text{OH})^+$, $\text{TcO}(\text{OH})_2(\text{aq})$

and $\text{TcO}(\text{OH})_3^-$ as the hydrolysis species controlling the aqueous chemistry of Tc(IV) from acidic to hyperalkaline pH conditions in the absence of strong complexing ligands. No activity model (SIT ion interaction parameters) was provided for these species due to the lack of experimental studies at elevated ionic strength. This thermodynamic model was recently updated by Yalcintas and co-workers, who conducted a comprehensive solubility study with Tc(IV) in dilute to concentrated NaCl, MgCl_2 and CaCl_2 solutions.⁹ Based on the combination of their own experimental data with available spectroscopic evidence,^{10–13} the authors proposed the predominance of $\text{Tc}_3\text{O}_5^{2+}$ in the acidic pH region (instead of TcO^{2+} and $\text{TcO}(\text{OH})^+$), but retained $\text{TcO}(\text{OH})_2(\text{aq})$ and $\text{TcO}(\text{OH})_3^-$ as the main aqueous species prevailing under near-neutral and alkaline pH-conditions, respectively. The study by Yalcintas *et al.* (2016) also shows that Tc(IV) solubility behavior in the alkaline pH region is significantly affected by ionic strength as well as the counter ions present in the system. Unlike sodium, Mg- and Ca-containing systems showed a steep increase in Tc(IV) solubility above $\text{pH}_m = 8$ and 9.5 , respectively, due to the formation of two previously unreported ternary $\text{Mg}_3/\text{Ca}_3[\text{TcO}(\text{OH})_5]^{3+}$ species.

In spite of the relevance of potassium in certain environments related to nuclear waste disposal, thermodynamic and activity models for Tc(IV) in KCl systems are still lacking. This is especially important for alkaline pH conditions, where ion-interaction processes of the predominant anionic species $\text{TcO}(\text{OH})_3^-$ with K^+ are expected to impact the solubility of Tc. In this framework, the present study investigates the solubility of Tc(IV) in dilute to concentrated KCl solutions across the entire pH range in order to derive the corresponding thermodynamic data and activity models to be implemented in thermodynamic databases and geochemical calculations. In a second step of our study, Tc(IV) solubility experiments are performed in simulated groundwater/pore water compositions of relevance in the context of nuclear waste disposal with the intent of validating the applicability of the chemical, thermodynamic and activity models derived in this work and in Yalcintas *et al.* (2016) for the system $\text{Tc}^{4+}-\text{H}^+-\text{K}^+-\text{Na}^+-\text{Mg}^{2+}-\text{Ca}^{2+}-\text{OH}^--\text{Cl}^--\text{H}_2\text{O}(\text{l})$.⁹

2. Experimental

2.1. Chemicals

KCl (p.a.), NaCl (p.a.), $\text{MgCl}_2 \cdot 6\text{H}_2\text{O}$ (p.a.), $\text{CaCl}_2 \cdot 2\text{H}_2\text{O}$ (p.a.), $\text{Na}_2\text{S}_2\text{O}_4$ (p.a.), CHCl_3 (p.a.), KOH (Titrisol[®]), NaOH (Titrisol[®]) and HCl (Titrisol[®]) were purchased from Merck. TPPC ($\text{C}_{24}\text{H}_{20}\text{ClP}$, 98%), HEPES ($\text{C}_8\text{H}_{18}\text{N}_2\text{O}_4\text{S}$, $Z = 99.5\%$) and SnCl_2 (98%) were purchased from Sigma-Aldrich. Ethanol (99%) was purchased from VWR Chemicals. Perkin Elmer Ultima Gold[®] XR was used as liquid scintillation counting (LSC) cocktail.

All sample preparation and handling were performed in an Ar-glovebox ($\text{O}_2 < 1$ ppm) at $T = (22 \pm 2)$ °C. All solutions were prepared with ultrapure water purified using a Millipore Milli-Q Advantage A10 (18.2 MΩ cm at 25 °C, 4 ppb TOC) with Millipore Millipak[®] 40 0.22 μm and then purged with Ar for 1 hour before use to remove traces of oxygen and carbon dioxide.

2.2. pH and E_h measurements

All pH measurements were performed at $T = (22 \pm 2)$ °C using a ROSS combination pH electrode (Orion). Calibration prior to pH measurement was performed using pH standard buffer solutions (pH 1 to 13, Merck). In salt solutions of ionic strength $I_Z = 0.1$ mol kg⁻¹, the measured pH value (pH_{exp}) is an operational apparent value related to the molal proton concentration $[\text{H}^+]$ by $\log[\text{H}^+] = \text{pH}_m = \text{pH}_{\text{exp}} + A_m$ (and molar proton concentration by $\log[\text{H}^+] = \text{pH}_c = \text{pH}_{\text{exp}} + A_c$, respectively),^{14,15} where A_m (A_c) is an empirical correction factor.

A_m values for KCl systems are not available in the literature and were derived experimentally in the present work (p.w.) for 0.1, 0.25, 0.5, 2.0, 3.0 and 4.0 M (or otherwise 0.1, 0.25, 0.51, 2.13 and 4.58 m) KCl solutions. A set of reference samples containing well-defined mixtures of HCl and KCl (with 2×10^{-2} mol kg⁻¹ $[\text{H}^+] \approx 6.25 \times 10^{-4}$ M) were prepared and successively mixed with a KCl solution of the same ionic strength. The pH_{exp} of each dilution step was measured and compared to the known $[\text{H}^+]$ resulting in the respective empirical correction factors A_m .

The A_m values for other concentrations are derived through second-grade polynomial fitting of the experimentally determined A_m -factors for KCl solutions according to

$$A_m = B_0 + [j]B_1 + [j]^2B_2 \quad (1)$$

with $[j]$ as the molality of ions j and yielding A_m values for KCl:

$$A_m(\text{KCl}) = 0.1597 + 0.0132[\text{KCl}] + 0.0204[\text{KCl}]^2 \quad (2)$$

A_m values for NaCl, MgCl_2 and CaCl_2 systems were taken from Altmaier *et al.* (2003, 2008).^{16,17} A comparison of A -factors of different salts in aqueous solution is shown in Fig. 7 in the Appendix. Note that A -factors in salt-mixtures are additive and can be calculated according to

$$A_m^{\text{mix}} = B_0^{\text{mix}} + m_j B_1^{\text{mix}} + m_j^2 B_2^{\text{mix}} \quad (3)$$

$$B_n^{\text{mix}} = \left[B(\text{KCl}) \cdot \left(\frac{[\text{K}^+]}{[\text{Cl}^-]} \right) \right] + \left[B(\text{NaCl}) \cdot \left(\frac{[\text{Na}^+]}{[\text{Cl}^-]} \right) \right] + \left[B(\text{MgCl}_2) \cdot \left(\frac{2[\text{Mg}^{2+}]}{[\text{Cl}^-]} \right) \right] + \left[B(\text{CaCl}_2) \cdot \left(\frac{2[\text{Ca}^{2+}]}{[\text{Cl}^-]} \right) \right] \quad (4)$$

In KCl-KOH solutions with $[\text{OH}^-] = 0.03$ M, the proton concentration was calculated using g_{H^+} , g_{OH^-} (as calculated by SIT) and the activity of water ($a_{\text{H}_2\text{O}}$), at each ionic strength, as reported in the NEA-TDB.⁷ In MgCl_2 and CaCl_2 solutions, the highest pH_m (pH_{max}) is fixed by the precipitation of $\text{Mg}(\text{OH})_2(\text{s})$ and $\text{Ca}(\text{OH})_2(\text{s})$ (or the corresponding hydroxochlorides at Ca/Mg concentrations above $E = 2$ m), which buffer pH_m at $E = 9$ and $E = 12$, respectively.¹⁶

E_h measurements were performed with Pt combination electrodes with Ag/AgCl reference system (Metrohm) and converted to E_h (redox potential *versus* the standard hydrogen electrode) by correction for the potential of the Ag/AgCl reference electrode (+208 mV for 3 M KCl at 22 °C). All samples were measured for 15–30 minutes. Note that agitation was applied in

those samples with heterogeneous reducing systems (*e.g.* participation of a solid phase in redox buffering). The apparent electron activity ($pe = -\log a_e$) was calculated from $pe = 16.9E_h$ [V], according to the equation $E_h = \frac{RT \ln 10}{F} \log a_e$. The redox electrode was tested with a standard redox buffer solution (Schott, +220 mV vs. Ag/AgCl) and provided readings within ± 10 mV of the certified value.

2.3. Determination of Tc total concentration and redox speciation in solution

Liquid scintillation counting (LSC) was used to quantify the total concentration of Tc in the aqueous phase after ultrafiltration using 10 kD filters (2–3 nm cut-off, Nanosep[®] and Mikrosep[®] Pall Life Sciences) to separate colloids or suspended solid phase particles. The filtrate was acidified with 600 μ l of 1 M HCl, added into 10 ml of LSC cocktail (Perkin Elmer Ultima Gold[®] XR) in a screw cap vial (PP, 20 ml, Zinsser Analytic) and measured using an LKB Wallac 1220 Quantulus Liquid Scintillation Counter for 30 minutes each. The background count was determined by measuring inactive blanks and the resulting detection limit (3 standard deviations of the blank) was calculated as 7.9×10^{-10} M. Each sample was corrected to account for the radiation emitted by ⁴⁰K.

Liquid–liquid extraction (LLE) was used for the quantification of the redox speciation of Tc in the aqueous phase. After ultrafiltration using 10 kD filters, selected samples were added into the solutions of 50 mM TPPC in chloroform and shaken for 60 seconds, thereby extracting Tc(vii) to the organic phase.¹⁸ After subsequent separation of the aqueous and organic phases, the technetium concentration in the aqueous phase was determined by LSC and was attributed to the presence of Tc(iv).

2.4. Solubility experiments

Tc(iv) stock solution was prepared by electrochemical reduction of Tc(vii) in 1.0 M HCl at $E = 50$ mV vs. SHE under an Ar-atmosphere in a glovebox. The resulting Tc(iv) suspension was quantitatively precipitated as $TcO_2 \cdot xH_2O(s)$ in a strongly reducing 5 mM $Na_2S_2O_4$ solution at $pH_m = 12.5$, and aged for two months before starting solubility experiments.

2.4.1. Solubility experiments in dilute to concentrated KCl solutions. The solubility of Tc(iv) in 0.1, 0.5, 3.0 and 4.0 M (or otherwise 0.1, 0.51, 3.31 and 4.58 m) KCl was investigated from undersaturation conditions. Experimental samples were set up at pH_m values ranging from 1.5 to 14.5 resulting in a total

of 24 samples. The pH_m values were adjusted under conservation of the respective ionic strengths using HCl–KCl, KOH–KCl and HEPES–KCl (6.5 $\leq pH_m \leq 8$) mixed solutions. The final concentration of HEPES in the latter samples was 0.02 M. To ensure the stabilization of technetium in its tetravalent state and to avoid oxidation, 2 mM $SnCl_2$ or 2 mM $Na_2S_2O_4$ was added as a reductant for all samples at $pH_m \leq 11$ or, respectively, $pH_m \leq 11$ based on previous Tc(vii)/Tc(iv) redox studies in our research group.^{19,20} pH_m and E_h values of the prepared background electrolytes were measured after 2 weeks to ensure that stable pH_m values and the necessary reducing conditions for Tc(iv) had been reached. After confirmation that all solutions were properly pre-equilibrated, 2–3 mg of the precipitated and aged Tc(iv) solid were washed three times with 1 ml of the matrix solution and then added to 20 ml of the matrix solution in 50 ml screw cap centrifuge vials (Nalgene[®], Thermo Scientific). pH_m , E_h and Tc concentrations in the solubility samples were measured at regular time intervals for up to 500 days. Once equilibrium conditions were reached (constant pH_m and [Tc]), pH values of the selected samples were slightly shifted in pH to obtain additional data points in the solubility curve. Samples were shifted from pH regions of low Tc(iv) solubility to regions with increased solubility in order to preserve the undersaturation approach.

2.4.2. Solubility experiments in “simulated reference systems”.

Five “simulated reference systems” with complex salt mixtures were selected to experimentally validate the applicability of the Tc(iv) thermodynamic model derived in this work (KCl system) and in Yalcintas *et al.* (2016) (NaCl, $MgCl_2$ and $CaCl_2$ systems) to close-to-real systems. The systems chosen are relevant in the context of radioactive waste disposal and are shortly summarized below. The respective compositions are listed in Table 1. Note that the components of these simulated reference systems were limited to hydroxide and chloride, although other salts were also present in some cases (*i.e.* sulphate, silicate). To ensure the stabilization of technetium in its tetravalent state and to avoid oxidation, 2 mM $SnCl_2$ was added as a reductant for all samples. These samples were prepared following the same approach as described above for the KCl system. pH_m , E_h and Tc concentrations in the solubility samples were measured at regular time intervals as described in previous sections.

– Artificial cement pore water (ACW). The composition of this pore water is representative of fresh cement paste/materials after contact with low ionic strength solutions, where Na_2O and K_2O have not been washed out yet and control the

Table 1 Salt concentration (in molal units) and pH_m values considered for the “simulated reference systems”

Ref.	[KCl]	[KOH]	[NaCl]	[NaOH]	[$MgCl_2$]	[$CaCl_2$]	pH_m
Artificial cement pore water (ACW) ²		0.181		0.113			13.19 ^c
Cement L/ILW simulates exposed to NaCl brine ^{4 a}	0.614		5.641	0.027 ^b			13.33
Cement L/ILW simulates exposed to NaCl brine ^{4 a}	0.240		4.923	0.021 ^b			12.93
Canadian reference groundwater ^{21 a}	0.341		2.321		0.359	0.851	7.05
WIPP generic weep brine ^{5 a}	0.437		3.113		1.032		8.65

^a Reported concentrations decreased by 10% to avoid precipitation of saturated salts. ^b Calculated from experimentally reported pH_{exp} . ^c This value is normally reported as “pH = 13.3”, which corresponds to pH_{exp} .

pH of the cement interstitial water. The synthetic composition described in Wieland and Van Loon (2003) was considered for the preparation of the matrix solution “ACW” with $\text{pH}_m = 13.2$.²

– Cement L/ILW simulates exposed to concentrated NaCl brine solutions. The work by Bube *et al.* (2013) reporting on the long term (B20 years) equilibration of ordinary Portland cement (OPC) with NaCl brines was considered to extract the composition of these two simulated reference systems.⁴ pH_{exp} data provided by the authors were converted to pH_m data using the *A*-factors reported above.

– Groundwater representative of the Canadian Shield crystalline rock (Canadian SR-270). The NWMO (Canadian Nuclear Waste Management Organization) selected two different groundwater compositions to be used for the radionuclide solubility calculations in Duro *et al.* (2010).²¹ The composition chosen in the present study is representative of a saline sedimentary groundwater. The pH reported for the system SR-270 (“pH = 5.8”) has been considered as pH_{exp} .

– WIPP generic weep brine (WIPP-GWB). GWB is a magnesium rich synthetic brine representing the average composition of intergranular fluids from the Salado Formation at or near the stratigraphic horizon of the WIPP underground repository in New Mexico (USA).^{5,6}

2.5. Solid phase characterization

The solid phase of selected solubility samples at (i) 0.1 M KOH; (ii) 4.0 M KCl with $\text{pH}_m = 7$; and (iii) 4.0 M KCl-KOH with $\text{pH}_m = 14.5$ was characterized after attaining equilibrium conditions using X-ray diffraction (XRD), quantitative chemical analysis, scanning electron microscope - energy dispersive spectrometry (SEM-EDS) and thermogravimetric analysis (TG-DTA). Approximately 1 mg of the Tc(IV)-containing solid was washed three times with ethanol inside the Ar-glovebox to remove the salt-containing matrix solution. The washed solid was suspended in E 10 mL of ethanol and transferred to the XRD sample plate and measured after the evaporation of ethanol. Measurements were performed on a Bruker AXS D8 Advance X-ray powder diffractometer (Cu- K_α radiation) at measurement angles $2\theta = 10\text{--}78^\circ$ with incremental steps of 0.0151 and a measurement time of 1.7 seconds per increment. After the measurement, the solid phase was dissolved in 1 ml of 3% HNO_3 and transferred for quantitative chemical analysis. The dissolved solid Tc phase was analysed by LSC and ICP-OES (inductively coupled plasma - optical emission spectroscopy) to determine the concentration of technetium and potassium, respectively. ICP-OES measurements were performed using a PerkinElmer OPTIMA 2000t. A second fraction of the washed solid was characterized by SEM-EDS (FEI Quanta 650 FEG equipped with a Noran EDS unit) for qualitatively assessing the morphology and particle size of the Tc(IV) solid phases.

Thermogravimetric analysis was performed to determine the number of hydration water molecules in the $\text{TcO}_2 \cdot x\text{H}_2\text{O}(\text{s})$ solid phase. The water content in the original Tc(IV) solid phase prepared by electrolysis was determined using a Netzsch STA 449C installed inside an Ar-glovebox. 8.7 mg of the Tc(IV) solid was washed 3 times with ethanol and left to dry for 3 days

under an Ar atmosphere. The measurements were performed by increasing the temperature by 5 K per minute up to a final temperature of 200 °C.

3. Results and discussion

3.1. Solid phase characterization

The very broad XRD patterns observed for the Tc(IV) solid in 0.1 M KOH (see Fig. 8 in Appendix) are analogous to those reported in dilute to concentrated NaCl solutions⁹ and can be attributed to $\text{TcO}_2 \cdot x\text{H}_2\text{O}(\text{s})$. Sharp features corresponding to KCl (PDF 73-0380) are observed in the solid phases equilibrated in 4.0 M (4.58 m) KCl, indicating that the washing step was insufficient to completely remove the KCl background electrolyte. Note however that similar broad features to those mentioned above can again be observed in the XRD of these samples, indicating the presence of amorphous $\text{TcO}_2 \cdot x\text{H}_2\text{O}(\text{s})$.

Three different solid phases can be identified in the selected SEM images shown in Fig. 9 in the Appendix, corresponding to Tc(IV) equilibrated in 4.0 M KCl at $\text{pH}_m = 7$. The crystalline structure “A” has been identified as KCl by EDS analysis in agreement with the predominant XRD pattern exhibited by this sample. The needle-like structure “B” corresponds to a tin-containing compound (likely $\text{Sn}(\text{OH})_2(\text{s})$) added in this sample to fix strongly reducing redox conditions, whereas Tc is the main component of the amorphous aggregates “C”. Neither potassium nor chlorine is identified by EDS in the latter aggregates, thus supporting the predominance of a Tc oxo-hydroxide solid phase. The examination of the solid sample in 0.1 M KOH, with $\text{Na}_2\text{S}_2\text{O}_4$ as a reducing chemical, again shows the amorphous aggregates corresponding to a Tc solid phase (Fig. 10). No needle-like structures appear in this case due to the absence of Sn. Instead, the submicrometer-sized particles observed in the SEM images are likely related to $\text{Na}_2\text{S}_2\text{O}_4$ or its potential degradation products. EDS data collected for concentrated KCl systems resulted in a ratio K:Cl = 1:1, confirming the presence of KCl found in the XRD measurements. Quantitative chemical analysis (LSC and ICP-OES) confirms also the presence of potassium in the Tc solid phases recovered from concentrated KCl solutions, in good agreement with XRD and SEM-EDS results.

The number of hydration water molecules was determined by thermogravimetric analysis (TG-DTA) and resulted in a degree of hydration of $x = (0.5 \pm 0.1)$. This finding agrees well with the number of hydration water molecules determined for $\text{TcO}_2 \cdot x\text{H}_2\text{O}(\text{s})$ solid phases equilibrated in NaCl, MgCl_2 and CaCl_2 solutions for a similar time frame, reported as $x = (0.6 \pm 0.3)$.⁹ In the following discussion, the solid phase controlling the solubility of Tc(IV) in the KCl system over the entire pH range is defined as $\text{TcO}_2 \cdot 0.6\text{H}_2\text{O}(\text{s})$.

3.2. Tc redox speciation

Liquid-liquid-extraction was performed for selected samples to assess the redox speciation of Tc in the aqueous phase after attaining equilibrium conditions. The results of these analyses

Table 2 Percentage of Tc(IV) determined by liquid-liquid extraction for the supernatant of selected Tc solubility samples. Errors: $\text{pH}_m \pm 0.05$, $E_h \pm 50$ mV, solvent extraction $\pm 10\%$

Reducing system	Background electrolyte	pH_m	E_h [mV]	$(\text{pe} + \text{pH}_m)$	Tc(IV) [%]
2 mM Sn(II)	3.0 M KCl	1.96	10	2.1	95
2 mM Sn(II)	4.0 M KCl	2.03	20	2.4	96
2 mM $\text{Na}_2\text{S}_2\text{O}_4$	0.1 M KOH	12.84	660	1.7	96
2 mM $\text{Na}_2\text{S}_2\text{O}_4$	0.5 M KOH	13.45	670	2.1	99
2 mM $\text{Na}_2\text{S}_2\text{O}_4$	2.0 M KCl + 1 M KOH	14.15	660	3.0	99
2 mM $\text{Na}_2\text{S}_2\text{O}_4$	3.0 M KCl + 1 M KOH	14.37	670	3.0	98

are summarized in Table 2, together with information on the reducing system used, $[\text{KCl}]$, pH_m , E_h and $(\text{pe} + \text{pH}_m)$ in each independent sample. As predicted by the combination of $(\text{pe} + \text{pH}_m)$ values and thermodynamic calculations, liquid-liquid extraction confirms the predominance of Tc(IV) in all the samples evaluated ($95\text{--}99 \pm 10\%$).

3.3. Solubility of Tc(IV) in dilute to concentrated KCl solutions

pH and E_h measurements confirmed that very reducing conditions ($\text{pe} + \text{pH}_m \approx 2$) were retained within the timeframe of the solubility experiments (≈ 500 days). These $(\text{pe} + \text{pH}_m)$ values are consistent with the predominance of Tc(IV) both in the aqueous and solid phases, as confirmed by liquid-liquid extraction. Experimental solubility data obtained in dilute to concentrated KCl systems are shown in Fig. 1 (0.1 M and 0.5 M KCl) and 2 (3.0 M and 4.0 M KCl), together with solubility data in NaCl systems previously reported under analogous ionic strength conditions.⁹ Both figures include the solubility curve of $\text{TcO}_2 \cdot 0.6\text{H}_2\text{O}(\text{s})$ calculated at $I = 0$ with the chemical and thermodynamic models summarized in Table 3 as an indicative “reference” line.

In the acidic pH region, the solubility of Tc(IV) decreases with a slope of -2 ($\log[\text{Tc(IV)}]$ vs. pH_m), agreeing well with the experimental data previously reported in dilute to concentrated NaCl solutions.⁹ The solubility in this region is strongly

impacted by ionic strength, showing an increase of more than 2 orders of magnitude between 0.1 and 4.0 M KCl. Slow kinetics was also observed in samples at $\text{pH}_m \approx 3$, and contact times of ≈ 6 months were needed to attain equilibrium conditions in this pH_m region. Note that similar observations made in concentrated NaCl systems were attributed to the slow kinetics of polymerization reactions.⁹ Based on the slope analysis, solid phase characterization and analogy with the NaCl case, the chemical reaction $\text{TcO}_2 \cdot 0.6\text{H}_2\text{O}(\text{s}) + 2/3\text{H}^+ \rightleftharpoons 1/3\text{Tc}_3\text{O}_5^{2+} + 2.8/3\text{H}_2\text{O}(\text{l})$ is proposed to control the solubility of Tc(IV) in this pH region. Note further that the chemical model in Yalcintas *et al.* (2016) was able to explain the experimental observations in acidic solutions with up to $[\text{Cl}^-] = 9.0$ M ($I = 13.5$ M). The same scheme is therefore retained in the present study, where significantly lower chloride concentrations and ionic strength conditions are used ($[\text{Cl}^-] = I = 4.0$ M) (Fig. 2).

In the weakly acidic to alkaline pH region, no ionic strength effect is observed and the solubility of Tc(IV) shows pH-independent behavior. This can be explained by the predominance of the neutral species $\text{TcO}(\text{OH})_2(\text{aq})$ in the aqueous phase, in agreement with the NEA-TDB and further confirmed by Yalcintas *et al.* (2016). The data points in this pH region show a relatively large scattering. This behavior is likely caused by a combination of the low solubility of Tc(IV) and the tendency of neutral species to sorb and form colloidal species that may interfere in the process of phase separation.^{9,22,23}

Above $\text{pH}_m \approx 10$ (depending upon KCl concentration), the solubility of Tc(IV) increased with a well-defined slope of $+1$ ($\log[\text{Tc(IV)}]$ vs. pH_m) both in dilute and concentrated KCl systems. This is in excellent agreement with previous experimental observations,^{9,24} and corresponds to solubility-control by the chemical reaction $\text{TcO}_2 \cdot 0.6\text{H}_2\text{O}(\text{s}) + 1.4\text{H}_2\text{O}(\text{l}) \rightleftharpoons \text{TcO}(\text{OH})_3^- + \text{H}^+$. The solubility of Tc(IV) in this pH region decreases with increasing ionic strength by about one order of magnitude as a result of ion-interaction processes of the anionic species $\text{TcO}(\text{OH})_3^-$ with K^+ . In this pH_m region, equilibrium was attained after 4–10 weeks.

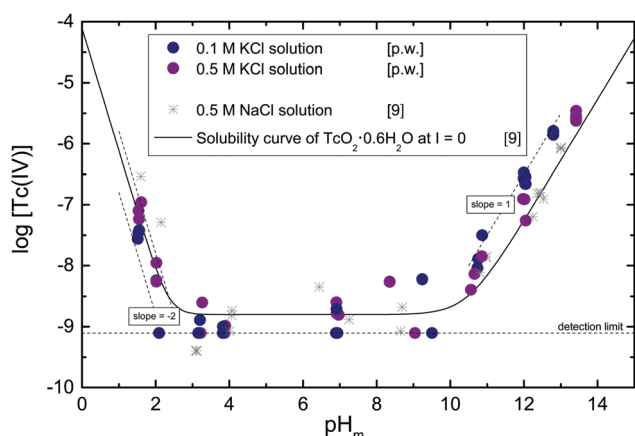


Fig. 1 Experimental solubility data of Tc(IV) in 0.1 M and 0.5 M KCl systems [p.w.] together with solubility data in 0.5 M NaCl as reported in Yalcintas *et al.* (2016). Solid line corresponds to the calculated solubility at $I = 0$ using the chemical and thermodynamic models summarized in Table 3.

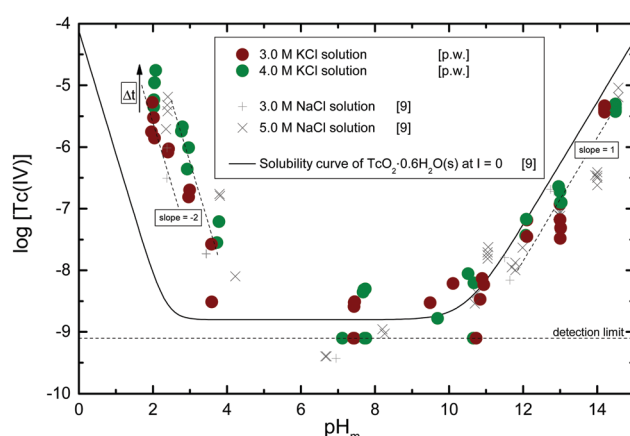


Fig. 2 Experimental solubility data of Tc(IV) in 3.0 M and 4.0 M KCl systems [p.w.] together with solubility data in 3.0 M and 5.0 M NaCl as reported in Yalcintas *et al.* (2016). Solid line corresponds to the calculated solubility at $I = 0$ using the chemical and thermodynamic models summarized in Table 3.

Table 3 Aqueous technetium species and stability constants derived in present work and reported in Yalcintas *et al.* (2016)

Reactions	SIT log *Kf	Pitzer log *Kf	Ref.
$\text{TcO}_2 \cdot 0.6\text{H}_2\text{O}(\text{s}) + 0.4\text{H}_2\text{O}(\text{l}) \rightleftharpoons \text{TcO}(\text{OH})_2(\text{aq})$	(8.8 ± 0.5)	(8.8 ± 0.5)	9
$\text{TcO}_2 \cdot 0.6\text{H}_2\text{O}(\text{s}) + \frac{2}{3}\text{H}^+ \rightleftharpoons \frac{1}{3}\text{Tc}_3\text{O}_5^{2+} + \frac{2.8}{3}\text{H}_2\text{O}(\text{l})$	(1.5 ± 0.2)	(1.5 ± 0.1)	9
$\text{TcO}_2 \cdot 0.6\text{H}_2\text{O}(\text{s}) + 3\text{Mg}^{2+} + 3.4\text{H}_2\text{O}(\text{l}) \rightleftharpoons \text{Mg}_3[\text{TcO}(\text{OH})_5]^{3+} + 3\text{H}^+$	(40.6 ± 0.5)	(40.3 ± 0.5)	9
$\text{TcO}_2 \cdot 0.6\text{H}_2\text{O}(\text{s}) + 3\text{Ca}^{2+} + 3.4\text{H}_2\text{O}(\text{l}) \rightleftharpoons \text{Ca}_3[\text{TcO}(\text{OH})_5]^{3+} + 3\text{H}^+$	(41.5 ± 0.3)	(41.7 ± 0.2)	9
$\text{TcO}_2 \cdot 0.6\text{H}_2\text{O}(\text{s}) + 1.4\text{H}_2\text{O}(\text{l}) \rightleftharpoons \text{TcO}(\text{OH})_3^- + \text{H}^+$	(19.27 ± 0.06) (19.0 ± 0.2)	(19.32 ± 0.10) (19.0 ± 0.2)	9 [p.w.]

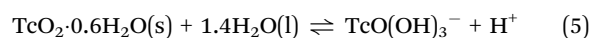
3.4. Thermodynamic model for the solubility and hydrolysis of Tc(IV) in KCl systems with $\text{pH}_m = 1.5 - 14.5$

The solubility and hydrolysis of Tc(IV) were comprehensively reviewed in the NEA-TDB series.^{7,8} Recently, Yalcintas *et al.* (2016) updated the chemical, thermodynamic and activity models of Tc(IV) in NaCl, MgCl₂ and CaCl₂ systems based on new solubility data and spectroscopic evidence previously reported in the literature.⁹ The chemical model proposed in the latter study is in excellent agreement with the experimental observations and slope analysis obtained in the present study. Therefore, the hydrolysis scheme proposed by the authors for the acidic pH-range, where only interactions with the commonly used Cl⁻ anion are expected, is also adopted here. In weakly acidic to weakly alkaline pH conditions, our experimental solubility data are in excellent agreement with $\log K_{s,\text{TcO}(\text{OH})_2(\text{aq})}^{\circ} = 8.8$ reported in Yalcintas *et al.* (2016) for the solubility reaction $\text{TcO}_2 \cdot 0.6\text{H}_2\text{O}(\text{s}) + 0.4\text{H}_2\text{O}(\text{l}) \rightleftharpoons \text{TcO}(\text{OH})_2(\text{aq})$. Note that $\log K_{s,\text{TcO}(\text{OH})_2(\text{aq})}^{\circ}$ reported by the latter authors is 0.4 log-units lower than the value currently selected in the NEA-TDB. Such a difference is likely related to different numbers of hydration water molecules: 1.6 in the solid phase selected in the NEA-TDB corresponding to a fresh precipitate and 0.6 in the present work and in Yalcintas *et al.* (2016) corresponding to an aged phase.⁷⁻⁹ Equilibrium constants and ion interaction coefficients for both SIT and Pitzer determined in the present work and reported in Yalcintas *et al.* (2016) for Tc(IV) solubility and hydrolysis species are summarised in Tables 3 and 4, respectively.

For alkaline conditions where the anionic species $\text{TcO}(\text{OH})_3^-$ is expected to form, the unknown interaction parameters for ($\text{TcO}(\text{OH})_3^-$, K^+) are derived in the next section by extrapolating the conditional solubility constants to $I = 0$ using both the SIT and Pitzer approaches.²⁵⁻²⁷

3.4.1. Thermodynamic and activity models for $\text{TcO}(\text{OH})_3^-$ in KCl systems. The increase in solubility with a slope of

+1 ($\log[\text{Tc}(\text{IV})]$ vs. pH_m) in alkaline KCl systems is consistent with the chemical equilibrium reaction



and the corresponding equations for the calculation of $\log^* K'_{s,\text{TcO}(\text{OH})_3}$ and $\log^* K_{s,\text{TcO}(\text{OH})_3}^{\circ}$

$$\log^* K'_{s,\text{TcO}(\text{OH})_3} = \log[\text{TcO}(\text{OH})_3^-] - \text{pH}_m \quad (6)$$

$$\log^* K_{s,\text{TcO}(\text{OH})_3}^{\circ} = \log^* K'_{s,\text{TcO}(\text{OH})_3} + \log g_{\text{TcO}(\text{OH})_3} + \log g_{\text{H}^+} - 1.4 \log a_{\text{H}_2\text{O}} \quad (7)$$

The conditional solubility constants $\log^* K'_{s,\text{TcO}(\text{OH})_3}$ were determined according to eqn (7) based on the experimental solubility data obtained in 0.1, 0.5, 3.0 and 4.0 M KCl. SIT and Pitzer approaches are used in the following sections to develop the activity model for $\text{TcO}(\text{OH})_3^-$ in the KCl system.

SIT. The specific ion interaction theory (SIT) approach based on the extended Debye-Hückel law is recommended in the NEA-TDB up to $I_m \leq 3.5$ m. The activity coefficient of an ion j is defined by SIT as

$$\log g_j = -z_j^2 D + \sum_k e(j, k) [k] \quad (8)$$

where z_j is the charge of the ion j , D is the Debye-Hückel term $\left(D = \frac{A\sqrt{I_m}}{(1 + Ba_j\sqrt{I_m})} \right)$, $e(j, k)$ is the specific ion interaction coefficient of the ion j with the counter-ion k of the background electrolyte and $[k]$ is the molality of the ion k . Combining eqn (7) and (8), the values of $\log^* K_{s,\text{TcO}(\text{OH})_3}^{\circ}$ and \mathbf{De} can be calculated by

Table 4 SIT and Pitzer parameters derived in present work and reported in Yalcintas *et al.* (2016)

c	a	Pitzer				C^F	SIT	Ref.
		$b^{(0)}$	$b^{(1)}$	$b^{(2)}$	$e(i, j)$			
$\text{Tc}_3\text{O}_5^{2+}$	Cl	0.3681	2.697	0	0.0063	(0.41 ± 0.05)	9	
Na^+	$\text{TcO}(\text{OH})_3$	0.0087	0.3	0	0.035	(0.09 ± 0.02)	9	
Ca^{2+}	$\text{TcO}(\text{OH})_3$	0.3	1.7	0	0	0.15	9	
K^+	$\text{TcO}(\text{OH})_3$	0.2317	0.3	0	0	(0.17 ± 0.05)	[p.w.]	
$\text{Ca}_3[\text{TcO}(\text{OH})_5]^{3+}$	Cl	0.074	4.3	0	0.015	(0.37 ± 0.1)	9	
$\text{Mg}_3[\text{TcO}(\text{OH})_5]^{3+}$	Cl	0.074	4.3	0	0.015	(0.37 ± 0.1)	9	

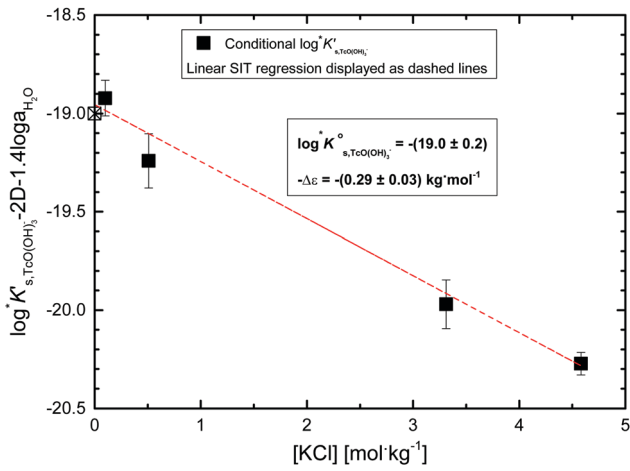


Fig. 3 SIT plot for the solubility reaction $\text{TcO}_2 \cdot 0.6\text{H}_2\text{O}(\text{s}) + 1.4\text{H}_2\text{O}(\text{l}) \rightleftharpoons \text{TcO}(\text{OH})_3 + \text{H}^+$ considering the conditional $\log^* K'_{s,\text{TcO}(\text{OH})_3}$ determined in dilute to concentrated KCl solutions.

linear regression of $\left(\log^* K'_{s,\text{TcO}(\text{OH})_3} - 2D - 1.4 \log a_{\text{H}_2\text{O}}\right)$ vs. $[\text{KCl}]$ as shown in eqn (9) and plotted in Fig. 3.

$$\begin{aligned} \log^* K'_{s,\text{TcO}(\text{OH})_3} - 2D - 1.4 \log a_{\text{H}_2\text{O}} \\ = \log^* K^{\circ}_{s,\text{TcO}(\text{OH})_3} - \text{De} \cdot [\text{KCl}] \end{aligned} \quad (9)$$

where

$$\text{De} = [\epsilon(\text{TcO}(\text{OH})_3^-, \text{K}^+) + \epsilon(\text{H}^+, \text{Cl}^-)] \quad (10)$$

The intercept obtained by linear SIT regression of the experimental data (dashed line) represents the $\log^* K^{\circ}$ value and gives a rounded value $\log^* K^{\circ}_{s,\text{TcO}(\text{OH})_3} = -(19.0 \pm 0.2)$. This value agrees within the uncertainties with $\log^* K^{\circ}_{s,\text{TcO}(\text{OH})_3}$ determined by Yalcintas and co-workers in NaCl systems.⁹ The slope of the linear SIT regression corresponds to $\text{De} = \epsilon(\text{TcO}(\text{OH})_3^-, \text{K}^+) - \epsilon(\text{H}^+, \text{Cl}^-)$, leading to $\epsilon(\text{TcO}(\text{OH})_3^-, \text{K}^+) = (0.17 \pm 0.08) \text{ kg mol}^{-1}$ considering $\epsilon(\text{H}^+, \text{Cl}^-) = (0.12 \pm 0.01) \text{ kg mol}^{-1}$ as reported in Guillaumont *et al.* (2003).⁸ This value is in moderate agreement with the SIT ion interaction coefficient reported for $\epsilon(\text{TcO}(\text{OH})_3^-, \text{Na}^+) = (0.09 \pm 0.02) \text{ kg mol}^{-1}$. Note that both KCl and NaCl systems have a large and positive value of De for the chemical reaction (5) (0.29 ± 0.03 for KCl (p.w.) and 0.21 ± 0.02 for NaCl⁹), which is correlated with a decrease of $\log^* K^{\circ}_{s,\text{TcO}(\text{OH})_3}$ with increasing ionic strength.

Pitzer approach. The Pitzer model is a system of equations which is suitable to calculate the interactions of ions in mixed electrolytes up to very high ionic strengths.^{26,28,29} The binary parameters $\mathbf{b}_{\text{ca}}^{(0)}$, $\mathbf{b}_{\text{ca}}^{(1)}$, $\mathbf{b}_{\text{ca}}^{(2)}$, C_{ca}^{F} and the parameters $y_{\text{cc}'}$, $y_{\text{aa}'}$ hereby allow the consideration of binary ion interactions between cations c and anions a in model calculations, whilst $C_{\text{cc}'a}$ and $C_{\text{aa}'c}$ account for triple ion interactions of cations c , c' , anions a , a' etc. The full set of Pitzer equations can be found elsewhere.²⁶

Experimental $\log^* K'_{s,\text{TcO}(\text{OH})_3}$ values were fitted according to eqn (7) and using the Pitzer formalism for the calculation of $\mathbf{g}_{\text{TcO}(\text{OH})_3}$ and \mathbf{g}_{H^+} . The activity of water $a_{\text{H}_2\text{O}}$ and $\log \mathbf{g}_{\text{H}^+}$ were calculated using the Pitzer parameters reported in Harvie *et al.* (1984).²⁹ A number of simplifications and assumptions were

made to account for the limited number of experimental data (only four values of $\log^* K'_{s,\text{TcO}(\text{OH})_3}$) and to avoid overparametrization of the system. Hence, the binary parameter $\mathbf{b}^{(2)}$, C^{F} and the mixing parameters $y(\text{TcO}(\text{OH})_3^-, \text{Cl}^-)$ and $C(\text{TcO}(\text{OH})_3^-, \text{K}^+, \text{Cl}^-)$ were set equal to zero. The binary parameter $\mathbf{b}^{(1)}$ was set to 0.3 kg mol^{-1} based on charge analogies reported in Grenthe *et al.* (1997).³⁰ $\log^* K^{\circ}_{s,\text{TcO}(\text{OH})_3}$ and $\mathbf{b}_{s,\text{TcO}(\text{OH})_3, \text{K}^+}^{(0)}$ are fitted by minimizing the difference between experimental and calculated $\log^* K'_{s,\text{TcO}(\text{OH})_3}$ in 0.1 M, 0.5 M, 3.0 M and 4.0 M KCl systems, resulting in

$$\log^* K^{\circ}_{s,\text{TcO}(\text{OH})_3} = -(19.0 \pm 0.2)$$

$$\mathbf{b}_{s,\text{TcO}(\text{OH})_3, \text{K}^+}^{(0)} = 0.2317 \text{ kg mol}^{-1}$$

$$\mathbf{b}_{s,\text{TcO}(\text{OH})_3, \text{K}^+}^{(1)} = 0.3 \text{ kg mol}^{-1}$$

$$C_{s,\text{TcO}(\text{OH})_3, \text{K}^+}^{\text{F}} = 0$$

The values of $\log^* K^{\circ}_{s,\text{TcO}(\text{OH})_3}$ determined by SIT and Pitzer approaches are in excellent agreement. The value of $\mathbf{b}_{s,\text{TcO}(\text{OH})_3, \text{K}^+}^{(0)}$ resulting from the Pitzer fit is also in very good agreement with the estimated value calculated by the approach described by Grenthe *et al.* (1997) ($\mathbf{b}^{(0)} = 0.035 + \epsilon(\text{TcO}(\text{OH})_3^-, \text{K}^+) \cdot \ln(10)/2 = 0.23 \text{ kg mol}^{-1}$).³⁰ This agreement is also reflected in Fig. 4, which shows the experimental and calculated $\log^* K'_{s,\text{TcO}(\text{OH})_3}$ using both SIT and Pitzer activity models.

Fig. 5 shows a comparison of the experimental solubility data obtained in the present work in KCl systems and the calculated solubility curves using the thermodynamic and (SIT, Pitzer) activity models for the system $\text{Tc}^{4+}\text{-K}^+\text{-H}^+\text{-Cl}^-\text{-OH}^-\text{-H}_2\text{O}(\text{l})$ summarized in Tables 3 and 4. The agreement between thermodynamic calculations using both activity models and the experimentally determined solubility of Tc(IV) in KCl solutions is very good in all pH regions.

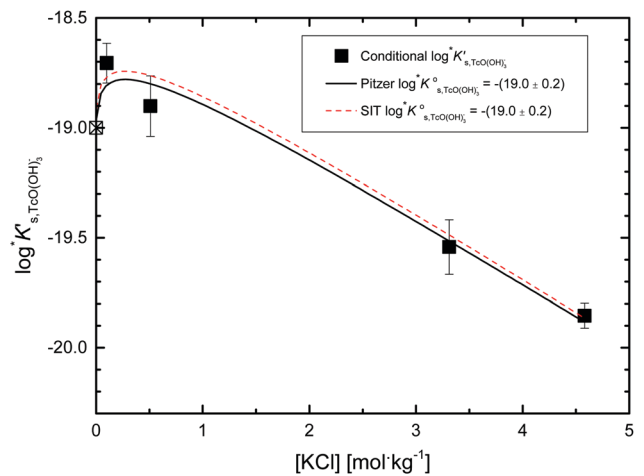


Fig. 4 Conditional equilibrium constants $\log^* K'_{s,\text{TcO}(\text{OH})_3}$ as a function of $[\text{KCl}]$: experimental values (symbols) and calculated fit based on the Pitzer (solid line) and the SIT approaches (dashed line).

3.5. Solubility of Tc(IV) in “simulated reference systems”

Five independent batch solubility samples were prepared from undersaturation conditions containing $\text{TcO}_2 \cdot 0.6\text{H}_2\text{O}(\text{s})$ with salt mixtures ($\text{NaCl-KCl-MgCl}_2\text{-CaCl}_2$) of given pH_m and I_m as summarized in Table 1.^{2,4,5,21} Tc(IV) experimental solubility data obtained for these “simulated reference systems” are shown in Fig. 6, together with the corresponding solubility curves calculated using the thermodynamic and Pitzer activity models summarized in Tables 3 and 4. The unweighted average of the $\log^* K_{s, \text{TcO}(\text{OH})_3}^\circ$ values obtained in the present work and in Yalcintas *et al.* (2016) was used in the calculations. The activity of water $a_{\text{H}_2\text{O}}$ was calculated using the Pitzer–Mayorga model. The values of $\log g_{\text{H}^+}$, $\log g_{\text{Mg}^{2+}}$ and $\log g_{\text{Ca}^{2+}}$ were calculated using the Pitzer parameters reported in Harvie *et al.* (1984).^{29,31,32} Thermodynamic calculations for these systems were performed based on the Pitzer approach using a self-programmed Microsoft Excel[®] file incorporating the original Pitzer equations as reported in Pitzer *et al.* for mixed salt systems,^{26,31,32} and counter-checked using The Geochemist’s Workbench[®] code.

The solubility of Tc(IV) in artificial cement pore water shows the highest Tc concentration of all the evaluated systems ($\approx 10^{-5.7}$ M), mostly due to the predominance in the solution of the anionic hydrolysis species $\text{TcO}(\text{OH})_3^-$. This observation is in good agreement with solubility data obtained in dilute KCl and NaCl systems as determined in this work and reported in Yalcintas *et al.* (2016). The two cement pore water compositions reported in Bube *et al.* (2013) are representative of NaCl-dominated saline systems. Fig. 6 shows very similar Tc concentrations for both samples ($10^{-6.5}$ – 10^{-7} M). As observed in pure KCl and also in pure NaCl solutions, the two cement pore water compositions (I_m E 5.2–6.3 m) follow the trend of decreasing solubility with increasing salt concentration when compared with the solubility of Tc(IV) in ACW (I_m E 0.3 m). The solubility of Tc(IV) in groundwater representative of the Canadian Shield crystalline rock SR-270 (0.303 M KCl + 2.065 M NaCl + 0.32 M MgCl_2 + 0.756 M CaCl_2) and the GWB simulated WIPP brine (0.414 M KCl + 2.723 M NaCl + 0.903 M MgCl_2) agree well with the very low solubility (10^{-7} M \leq $[\text{Tc(IV)}] \leq 10^{-9}$ M)

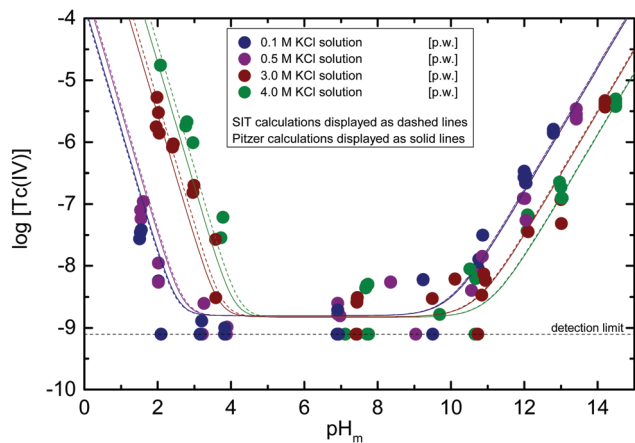


Fig. 5 Experimental solubility data of Tc(IV) in dilute to concentrated KCl systems (symbols) and calculated solubility curves using the thermodynamic and activity models (solid line: Pitzer; dashed line: SIT) summarized in Tables 3 and 4.

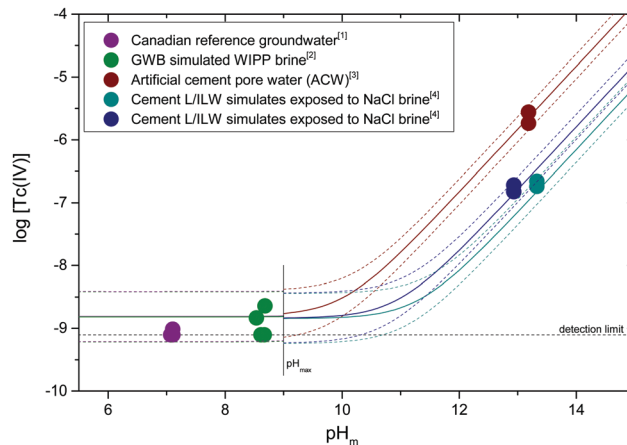


Fig. 6 Experimental solubility data of Tc(IV) in simulated reference systems (symbols) and solubility curves (solid lines) calculated with the thermodynamic and Pitzer activity models summarized in Tables 3 and 4. Dashed lines correspond to the uncertainties in the solubility calculations.

expected for $\text{TcO}_2 \cdot 0.6\text{H}_2\text{O}(\text{s})$ under near-neutral and weakly alkaline pH conditions.

Experimental solubility data determined for these “simulated reference systems” show excellent agreement with solubility calculations using the chemical, thermodynamic and activity models based on the recent work of Yalcintas *et al.* and the present study for the system $\text{Tc}^{4+}\text{-H}^+\text{-K}^+\text{-Na}^+\text{-Mg}^{2+}\text{-Ca}^{2+}\text{-OH}^-\text{-Cl}^-\text{-H}_2\text{O}(\text{l})$ as summarized in Tables 3 and 4. This provides an experimental validation to the use of thermodynamic models derived from simplified systems with single electrolytes in geochemical calculations with complex systems including mixed electrolytes. The available database allows reliable source term estimations for Tc solubility under conditions relevant in the context of radioactive waste disposal, which extend from dilute systems to concentrated mixed brines as those expected in rock-salt repositories. On-going experimental studies at KIT-INE will extend the model presented in the present work to carbonate containing aqueous systems in dilute to concentrated NaCl solutions.

4. Conclusions

A comprehensive study of the solubility of Tc(IV) in dilute to concentrated KCl solutions was performed under acidic to hyper-alkaline pH conditions. Solid phase characterization by XRD, SEM-EDS, quantitative chemical analysis and TG-DTA identified the solubility controlling solid phase as $\text{TcO}_2 \cdot 0.6\text{H}_2\text{O}(\text{s})$ in agreement with earlier studies in NaCl media. Redox speciation by liquid-liquid extraction confirmed the predominance of Tc(IV) aqueous species within the ($\text{pe} + \text{pH}_m$) and $[\text{KCl}]$ conditions considered in the present work. The chemical, thermodynamic and activity models recently reported in Yalcintas *et al.* (2016) explain the findings in KCl solutions in the acidic and neutral pH region very well. Above pH_m E 10, where the $\text{TcO}(\text{OH})_3^-$ species is predominant and interaction processes of this anionic species with the K^+ cation will govern ion interaction processes, both SIT and Pitzer approaches were used to determine thermodynamic data and activity models. The combination of the present work in KCl solutions with thermodynamic

data and activity models derived at KIT-INE for NaCl, MgCl₂ and CaCl₂ systems allows comprehensive, close-to-real geochemical calculations for systems directly relevant in the context of nuclear waste disposal. The experimental Tc(IV) solubility determined in five simulated reference systems shows excellent agreement with thermodynamic calculations using the above model for the systems $\text{Tc}^{4+}\text{-H}^+\text{-K}^+\text{-Na}^+\text{-Ca}^{2+}\text{-Mg}^{2+}\text{-OH}^-\text{-Cl}^-\text{-H}_2\text{O(l)}$. This outcome can be used as a direct input for the nuclear waste disposal Safety Case and highlights the importance of studying simplified aquatic systems and the related thermodynamics as fundamental building blocks for the accurate characterization of more complex systems.

Appendix

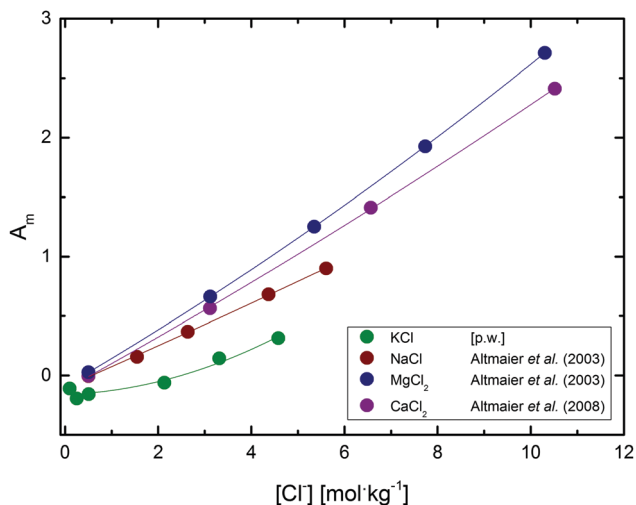


Fig. 7 Comparison of A factors of different salts in aqueous solution, as determined in the present work and reported in Altmaier *et al.* (2003, 2008).^{16,17}

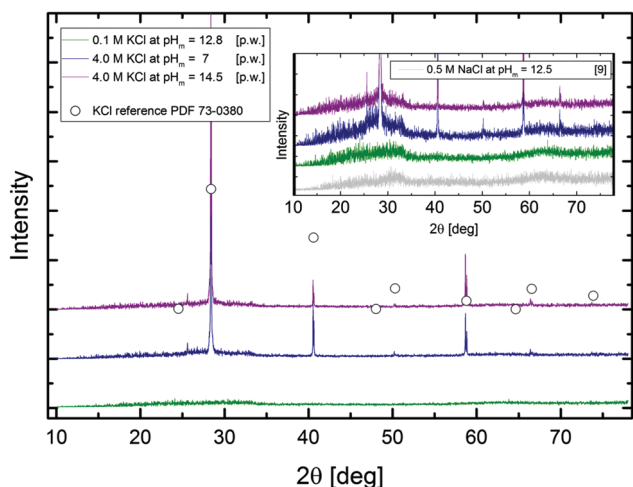


Fig. 8 XRD spectra collected for Tc(IV) solid phases contacted with 4.0 M KCl ($\text{pH}_m = 7$ and 14.5) and 0.1 M KOH ($\text{pH}_m = 12.8$). Inset corresponding to a zoom of the amorphous background. XRD spectra reported in Yalcintas *et al.* (2016) for $\text{TeO}_2 \cdot 0.6\text{H}_2\text{O(s)}$ equilibrated in 0.5 M NaCl appended in the inset for comparison.

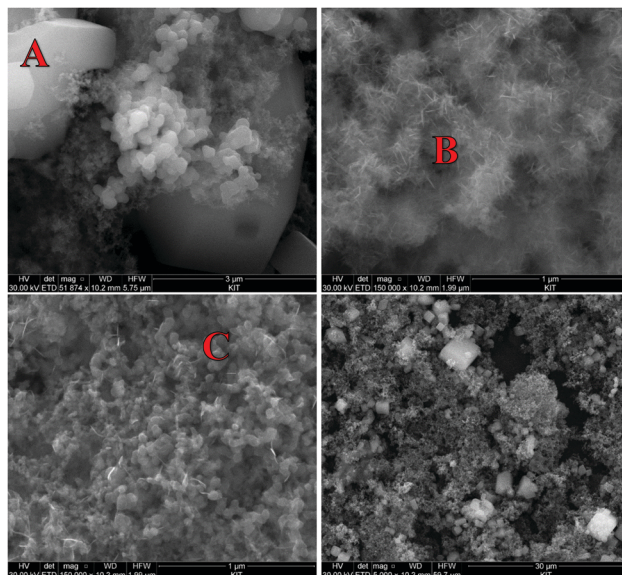


Fig. 9 SEM images of 4.0 M (4.58 m) KCl samples at $\text{pH}_m = 7$.

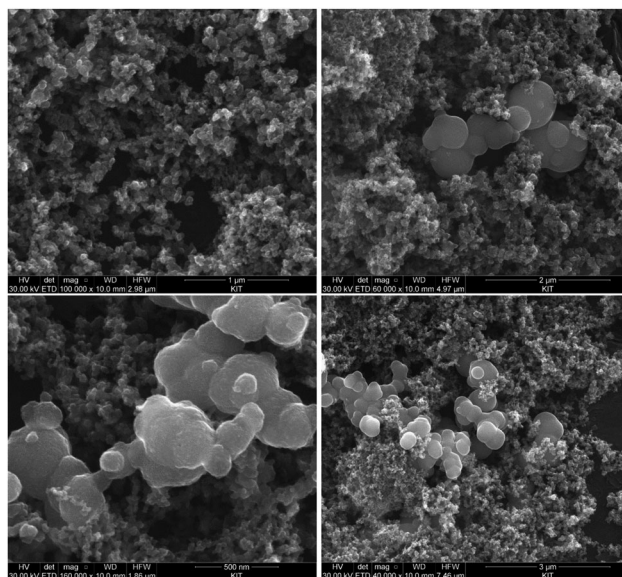


Fig. 10 SEM images of 0.1 M (0.1 m) KOH sample at $\text{pH}_m = 12.8$.

Conflicts of interest

There are no conflicts to declare.

Acknowledgements

The authors would like to thank M. Böttle, N. Finck, S. Heck, S. Moisei-Rabung and E. Soballa (KIT-INE) for their lab assistance and for performing XRD analyses, TG-DTA, ICP-OES and SEM-EDS.

References

- 1 B. Craeye, G. D. Schutter, H. V. Humbeeck and A. V. Cotthem, *Concrete containers for containment of vitrified high-level*

- radioactive waste: The Belgian approach*, Taylor & Francis Group, London, 2009.
- 2 E. Wieland and L. R. V. Loon, *Cementitious Near-Field Sorption Data Base for Performance Assessment of an ILW Repository in Opalinus Clay*, Paul Scherrer Institut, Villigen, Switzerland, 2003.
 - 3 H. F. W. Taylor, *Cement Chemistry*, Thomas Telford, 1997.
 - 4 C. Bube, V. Metz, E. Bohnert, K. Garbev, D. Schild and B. Kienzler, *Phys. Chem. Earth*, 2013, **64**, 87–94.
 - 5 J.-F. Lucchini, M. Borkowski, M. K. Richmanna, S. Ballard and D. T. Reeda, *J. Alloys Compd.*, 2007, 506–511.
 - 6 A. C. Snider, N. A. Wall, M. J. Chavez and D. S. Kessel, *Verification of the Definition of Generic Weep Brine and the Development of a Recipe for this Brine*, Sandia National Laboratories, Waste Isolation Pilot Plant, 2003.
 - 7 J. A. Rard, M. H. Rand, G. Anderegg and H. Wanner, *Chemical Thermodynamics of Technetium*, Elsevier, Amsterdam, 1999.
 - 8 R. Guillaumont, T. Fanghänel, J. Fuger, I. Grenthe, V. Neck, D. A. Palmer and M. H. Rand, *Update on the Chemical Thermodynamics of U, Np, Pu, Am and Tc*, Elsevier, Amsterdam, 2003.
 - 9 E. Yalcintas, X. Gaona, M. Altmaier, K. Dardenne, R. Polly and H. Geckeis, *Dalton Trans.*, 2016, **45**(21), 8916–8936.
 - 10 N. J. Hess, Y. Xia, D. Rai and S. D. Conradson, *J. Solution Chem.*, 2004, 33.
 - 11 L. Vichot, M. Fattahi, C. Musikas and B. Grambow, *Radiochim. Acta*, 2003, **91**, 263–271.
 - 12 L. Vichot, G. Oувrard, G. Montavon, M. Fattahi, C. Musikas and B. Grambow, *Radiochim. Acta*, 2002, **90**, 575–579.
 - 13 F. Poineau, M. Fattahi, C. D. Auwer, C. Hennig and B. Grambow, *Radiochim. Acta*, 2006, **94**, 283–289.
 - 14 K. G. Knauss, T. J. Wolery and K. J. Jackson, *Geochim. Cosmochim. Acta*, 1990, **54**, 1519–1523.
 - 15 V. Neck, M. Altmaier, R. Müller, V. Metz and B. Kienzler, *Experimentelles Programm zur Bestätigung der Ergebnisse von standortspezifischen Modellrechnungen für die Schachanlage Asse, Teil 3: Löslichkeitsexperimente zur Absicherung der thermodynamischen Datenbasis*, Forschungszentrum Karlsruhe, Insitute for Nuclear Waste Disposal (INE), 2003.
 - 16 M. Altmaier, V. Metz, V. Neck, R. Müller and T. Fanghänel, *Geochim. Cosmochim. Acta, Suppl.*, 2003, **67**, 3595–3601.
 - 17 M. Altmaier, V. Neck and T. Fanghänel, *Radiochim. Acta*, 2008, **96**, 541–550.
 - 18 R. Kopunec, F. N. Abudeab and S. Skragkovfi, *J. Radioanal. Nucl. Chem.*, 1998, **230**, 51–60.
 - 19 E. Yalcintas, X. Gaona, A. C. Scheinost, T. Kobayashi, M. Altmaier and H. Geckeis, *Radiochim. Acta*, 2015, **103**, 57–72.
 - 20 T. Kobayashi, A. C. Scheinost, D. Fellhauer, X. Gaona and M. Altmaier, *Radiochim. Acta*, 2013, **101**, 323–332.
 - 21 L. Duro, V. Montoya, E. Colàs and D. García, *Groundwater equilibration and radionuclide solubility calculations*, Nuclear Waste Management Organization, Toronto, Canada, 2010.
 - 22 V. Neck, M. Altmaier, T. Rabung, J. Lützenkirchen and T. Fanghänel, *Pure Appl. Chem.*, 2009, **81**, 1555–1568.
 - 23 M. Altmaier, V. Neck and T. Fanghänel, *Radiochim. Acta*, 2004, **92**, 537–543.
 - 24 T. E. Eriksen, P. Ndalamba, J. Bruno and M. Caceci, *Radiochim. Acta*, 1992, **58/59**, 67–70.
 - 25 E. A. Guggenheim and J. C. Turgeon, *Trans. Faraday Soc.*, 1955, **51**, 747–761.
 - 26 K. S. Pitzer, *J. Phys. Chem.*, 1972, **77**, 268–277.
 - 27 L. Ciavatta, *Ann. Chim.*, 1980, **70**, 551–567.
 - 28 C. E. Harvie and J. H. Weare, *Geochim. Cosmochim. Acta*, 1980, **44**, 981–997.
 - 29 C. E. Harvie, N. Moller and J. H. Weare, *Geochim. Cosmochim. Acta*, 1984, **48**, 723–751.
 - 30 I. Grenthe, A. V. Plyasunov and K. Spahiu, Estimations of Medium Effects on Thermodynamic Data, in *Modelling In Aquatic Chemistry*, OECD Publications, 1997, p. 724.
 - 31 K. S. Pitzer and G. Mayorga, *J. Phys. Chem.*, 1973, **77**, 2300–2308.
 - 32 K. S. Pitzer and G. Mayorga, *J. Solution Chem.*, 1974, **3**, 539–546.